The Relationship between the Microstructure and Engineering Properties of Hydroceramic Sealants for Geothermal Wells

K. Kyritsis[1], C. Hall[1], N. Meller[1], M. A. Wilson[2]

[1]School of Engineering & Electronics and Centre for Science at Extreme Conditions, The University of Edinburgh, Edinburgh, EH9 3JL UK;
[2]School of Mechanical, Aerospace & Civil Engineering, The University of Manchester, Manchester, M60 1QD, UK

1. Introduction

Cement is universally used in the construction of oil and geothermal wells. Cement slurries are placed primarily to secure and support the casing inside the well, but also to prevent entry of unwanted fluids into the well and communication between formation fluids at different levels [1]. These cements need to perform for many years at high temperatures and in severe chemical environments, such as brines or ground water containing carbon dioxide [1]. These substances can be aggressive towards the cement and reduce strength and increase permeability [2-4]; therefore it is necessary for cement formulations to be durable and resistant to chemical attack in order to seal the well for its working life.

Typical working temperatures for these wells are between 200 and 350 °C [1] and when the temperature exceeds 110 °C special cement formulations are used. There have been several recent attempts to design cements which are more durable at higher temperatures. Barlet-Gouédard et al. [5, 6] and Meller and Hall [7, 8] have designed slurries based on the $CaO–Al_2O_3–SiO_2–H_2O$ (CASH) system (cement nomenclature will be used in this paper C = CaO, S = SiO_2, A= Al_2O_3, H = H_2O). The aim is to develop formulations suitable for geothermal and deep, hot oil wells. These formulations contain minerals which occur in nature and may have the properties needed to be good well sealants. These are impermeability, strength and long-term stability in well environments. In particular, silica and alumina can be added to cement to produce CASH hydroceramics with a wide range of phases. A hydroceramic is defined here as any ceramic material containing chemically combined water as H_2O or OH or both [8].

The physical properties of cementitious materials required for such applications have been thoroughly investigated in the past [9-13] [14-16]. It is considered that the minimum compressive strength of the hardened slurry should be at least 7 MPa and the maximum permeability about 1×10^{-9} m s^{-1} (0.1 mD) [17]. Although much work has been done on the mechanical properties of these materials little is known about the relationship between these bulk properties and the microstructure of these

materials. The aim of this paper is to present the initial results of our work in this area.

2. Experimental procedure and techniques used

For our hydroceramic syntheses three reagents were used. Dyckerhoff oilwell cement (ISO Class G) was the basic component, used in all samples. This cement is widely used and has a consistent composition (Table 1). Silica flour HPF6 supplied by Sibelco and α-alumina (corundum) supplied by Sigma Aldrich were used as the sources of SiO_2 and Al_2O_3 respectively.

Oxides	Wt %
Na_2O	0.17
MgO	0.76
Al_2O_3	3.62
SiO_2	22.55
K_2O	0.66
CaO	65.61
TiO_2	0.17
Mn_3O_4	0.14
Fe_2O_3	4.53
SiO_2	1.82
Loss on ignition at 1000 ˚C	1.18
% Phases	By Rietveld refinement
Alite Ca_3SiO_5	66
Belite Ca_2SiO_4	17
Aluminoferrite Ca_2AlFeO_5	15

Table 1. Chemical and mineralogical analysis of Dyckerhoff Class G cement.

Two different sized specimens were made. To examine the mineralogy, small cylindrical PTFE cups were used, 2 cm dia and 1 cm deep. A total of 10 g of the three starting materials was weighed out in different proportions (Table 2) and 4 g of water added (w/s=0.4). For physical property measurements larger cups were used of the same diameter but 5 cm deep. Each sample was mixed by hand for approx 3 min and loaded into the appropriate cup. Small notches were cut in the rims of the PTFE cups to ensure a uniform water-saturated atmosphere. Twelve sample cups were placed in a stainless steel autoclave cell (type 4750 Parr Instruments) of 125 mL capacity with a pressure rating of 200 bar at the maximum working temperature of 350 °C. Once the Parr cells are closed they are placed in the oven at 200 °C and left to equilibrate for 5 days. The same procedure was followed for the samples cured at 250 °C.

After 5 days the cells were removed from the oven. Those containing samples to be used for the testing of physical properties were left to cool slowly in air to prevent cracking. The cells containing samples for X-ray analysis were quenched in cold water for 10 min. After drying in air the samples were removed from the cups. The smaller samples were milled and analysed by X-ray diffraction (XRD) using a Bruker AXS D8 diffractometer with monochromatic Cu-Kα radiation. A Braun position sensitive detector was used to collect data and the sample scanned over a $5–70^{o}$ 2θ range using a step size of 0.014^{o} and time per step of 0.3 s. The mineralogy of the samples cured at 200 °C is already known [8] and so only the analyses of the samples cured at 250 °C are reported here for the first time. However semi-quantitative Rietveld refinement using Bruker Topas software was carried out on samples cured at both 200 and 250 °C to estimate the percentage of phases present. This technique has only recently been applied to hydrated cement phases formed at elevated temperatures [18].

Sample composition by weight of cement (BWOC)	Curing temperature (°C)	Proportions (wt %)		
		Dyckerhoff cement	Silica flour HPF6	α-alumina
Pure cement	200	100	-	-
0.11 BWOC	200	90	10	-
0.43 BWOC	200	70	30	-
0.67 BWOC	200	60	40	-
1.00 BWOC	200	50	50	-
0.11 BWOC	200	90	-	10
0.43 BWOC	200	70	-	30
0.82 BWOC	200	55	-	45
0.11 BWOC	250	90	10	-
0.43 BWOC	250	70	30	-
0.67 BWOC	250	60	40	-

Table 2: List of samples examined.

A Philips XL30CP scanning electron microscope (SEM) with a PGT Spirit EDS analysis system was used to image and analyse the samples. All the samples were prepared as polished thin sections in order to be planar and relief free and were carbon coated. Thin sections enabled examination of the spatial distribution of the constituent phases in two dimensions as well as the nature of the boundaries between them.

Mechanical testing was performed with an Instron compression machine. A load of 50kN was applied with a loading rate of 0.33 mm min^{-1}. Compressive tests were carried out in accordance with ASTM C39-96 [19] on samples with an aspect ratio of 2. Two samples were tested for each

composition to check reproducibility. The compressive strength was calculated from the applied load at the point of sample failure.

Permeability tests were carried out using a purpose-built Hassler cell permeameter (Fig.1) [20]. This type of cell is widely used in petroleum technology [21]. The circumferential face of the specimen is sealed by pressurizing the water in the chamber surrounding a nitrile rubber sleeve fitted around the specimen. The confining pressure, which ensures axial flow of liquid through the specimen, is held constant throughout the experiment. The pressures of the confining liquid and the flow liquid (in this case water) are monitored. The system can measure pressures down to 0.1 MPa. Constant flow rate is maintained by means of a Gilson 307 chromatography pump.

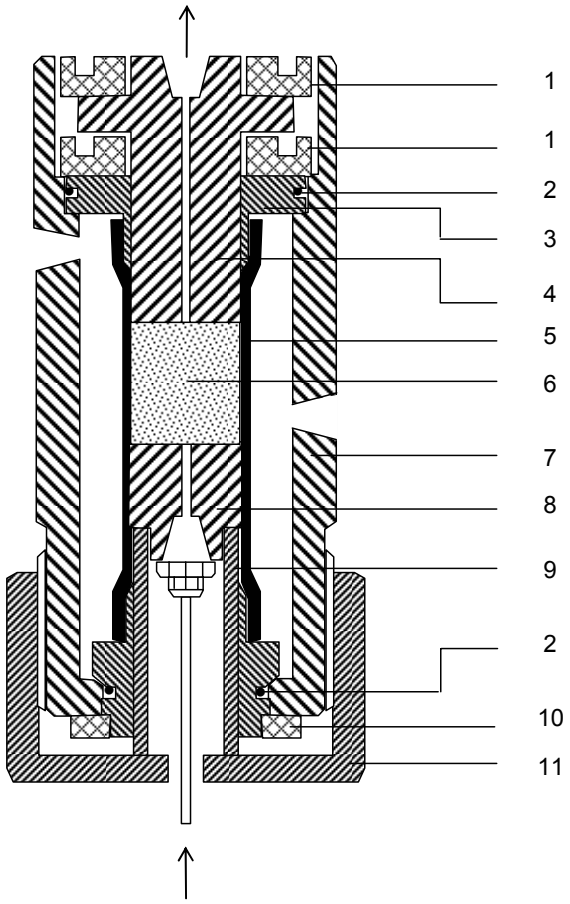

Fig. 1 Hassler cell permeameter after [21]: 1 Retaining ring; 2 nitrile rubber O-ring seal and PTFE back-up ring; 3 sleeve carrier; 4 fixed platen; 5 nitrile rubber sleeve; 6 sample; 7 stainless steel case; 8 movable platen; 9 platen carrier; 10 retaining ring; 11 end cap

Permeability test specimens, 22 mm dia × 25 mm length, were vacuum saturated with water before being loaded into the Hassler cell. The confining pressure was maintained at approximately 5 MPa. Simple Darcian flow was assumed and the saturated liquid conductivity (or conventional permeability), *K,* calculated from the equation $K = QL/PA$ *w*here *Q* is the steady volumetric flow rate through the sample of length *L* and cross-sectional area *A* at inlet gauge pressure *P*.

3. Results and discussion

3.1 Mineralogy

Several calcium silicate hydrates are formed in the pure cement sample cured at 200 °C. Quantitative analysis with Topas showed jaffeite $C_6S_2H_3$ as the major phase and portlandite CH along with α-dicalcium silicate hydrate α-C_2SH as the minor phases (Table 3). On adding 0.11 silica flour BWOC to the system, portlandite disappears and the anhydrous calcium silicate C_8S_5 is formed. The other phases are the same as in the pure cement system. For this sample the complexity of the diffraction pattern prevented a satisfactory quantitative phase refinement. Xonotlite C_6S_6H is the major phase formed when 0.43 silica BWOC is added. Traces of α-dicalcium silicate hydrate are detected. When the amount of silica flour is increased to 0.67 and 1.00 silica BWOC, truscottite $C_{14}S_{24}H_6$ forms at the expense of xonotlite. Unreacted quartz is found in the system with 1.00 silica flour BWOC.

Phases (wt %)	Sample composition (mineral additions by BWOC)										
	Cement	0.11	0.43	0.67	1.00	0.11	0.43	0.82	0.11	0.43	0.67
Jaffeite	71	*	-	-	-	31	10	8	47	-	-
Reinhardbraunsite	-	-	-	-	-	-	-	-	38	-	-
Calcium silicate C_8S_5	-	*	-	-	-	-	-	-	-	-	-
Xonotlite	-	-	98	33	10	-	-	-	13	86	15
9Å Tobermorite	-	-	-	-	-	-	-	-	-	14	12
Gyrolite	-	-	-	62	68	-	-	-	-	-	53
Truscottite	-	-	-	-	-	-	-	-	-	-	20
Hydrogarnet	-	*	-	-	-	63	75	57	2	-	-
Portlandite	9	-	-	-	-	6	-	-	-	-	-
α-Dicalcium silicate hydrate	20	*	2	-	-	-	-	-	-	-	-
Quartz	-	-	-	5	22	-	-	-	-	-	-
Corundum	-	-	-	-	-	-	15	35	-	-	-
Total	100	100	100	100	100	100	100	100	100	100	100

* Quantitative phase composition not refinable

Table 3: Phase composition in each sample

When alumina is added instead of silica flour the major phases at 0.11 alumina BWOC cured at 200 °C are hydrogarnet and jaffeite. Traces of portlandite are present. When increasing the proportion of alumina, hydrogarnet continues to be a major phase but unreacted alumina in the

form of corundum is also present. This type of alumina has been reported previously to be less reactive when added to the mix [18].

Diffraction analyses of the samples cured at 250 °C showed the presence of different calcium silicate hydration products to those produced at 200 °C (Table 3). The major phases for the system with 0.11 silica BWOC are reinhardbraunsite (also known as calcio-chondrodite) $C_5S_2H_2$ and jaffeite. Smaller amounts of xonotlite and hydrogarnet are also present. Increasing the percentage of silica to 0.43 BWOC resulted in xonotlite $C_6S_6H_2$ becoming the major phase and the appearance of 9Å tobermorite $C_5S_6H_5$. For 0.67 silica BWOC truscottite $C_{14}S_{24}H_6$ and gyrolite $C_4S_6H_4$ form and the minor phases appear to be xonotlite and 9Å tobermorite.

3.2 Microstructure

SEM images of three samples cured at 200 °C (cement only; silica 0.11 BWOC; 0.82 alumina BWOC) show that these materials are highly porous (Fig. 2). When silica is added to cement at 0.11 BWOC xonotlite is the dominant phase (Table 3) and appears as needle-like crystals (Fig. 2b). We show that when large amounts of alumina (0.82 BWOC) are added to cement corundum remains unreacted. This is illustrated in Fig. 2c by the dark grey crystals identified as corundum as identified by EDS.

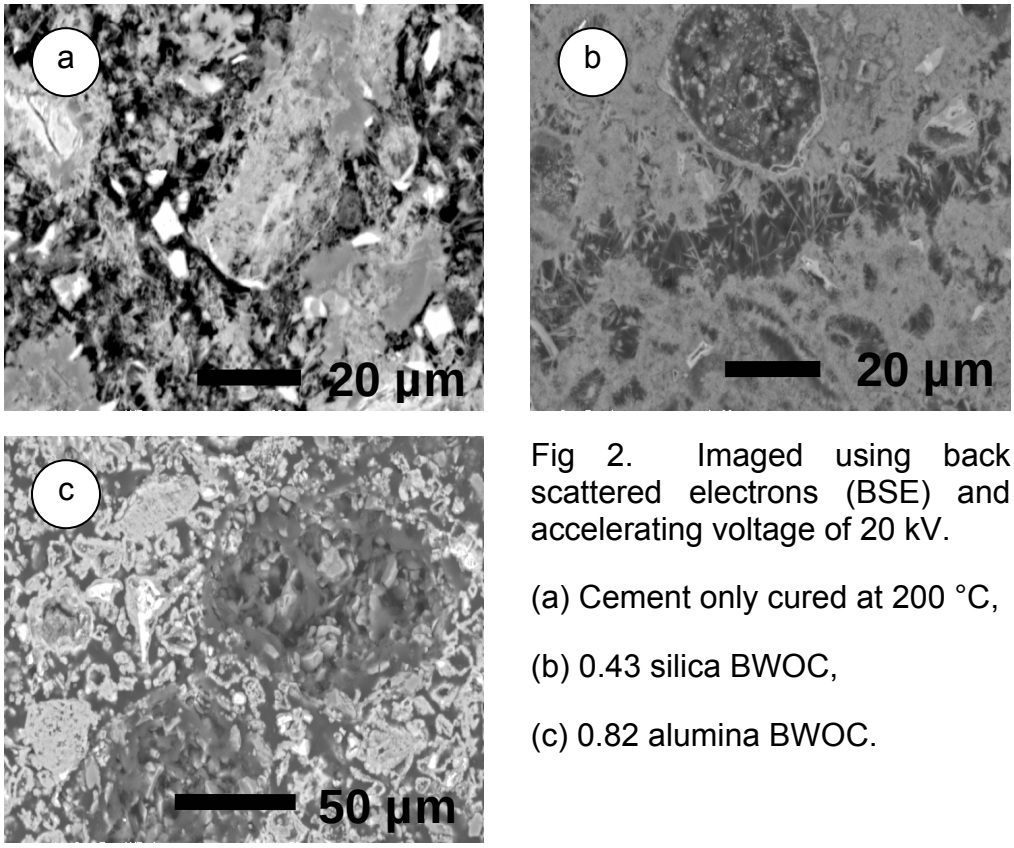

Fig 2. Imaged using back scattered electrons (BSE) and accelerating voltage of 20 kV.

(a) Cement only cured at 200 °C,

(b) 0.43 silica BWOC,

(c) 0.82 alumina BWOC.

3.3 Physical properties

The physical properties of the samples cured at 200 °C are improved by adding silica to the system as we observe an increase in the compressive strength and a decrease in permeability (Figs. 3 and 4). The results are in good agreement with Nelson and Barlet-Gouédard et al. [1, 22] and may be attributed to changes in mineralogy. The sample containing 0.43 silica BWOC shows improvements in both strength and impermeability, compared to pure cement, as different phases are present in each sample. Xonotlite, the major phase is probably responsible for this [15]. A further increase in silica (0.67 BWOC) produces a sample with gyrolite and this appear to reduce the strength. At 1.00 silica BWOC the same amount of gyrolite is present (Table 3) but the strength is increasing. Unreacted quartz crystals in the silica flour are probably responsible for this improvement.

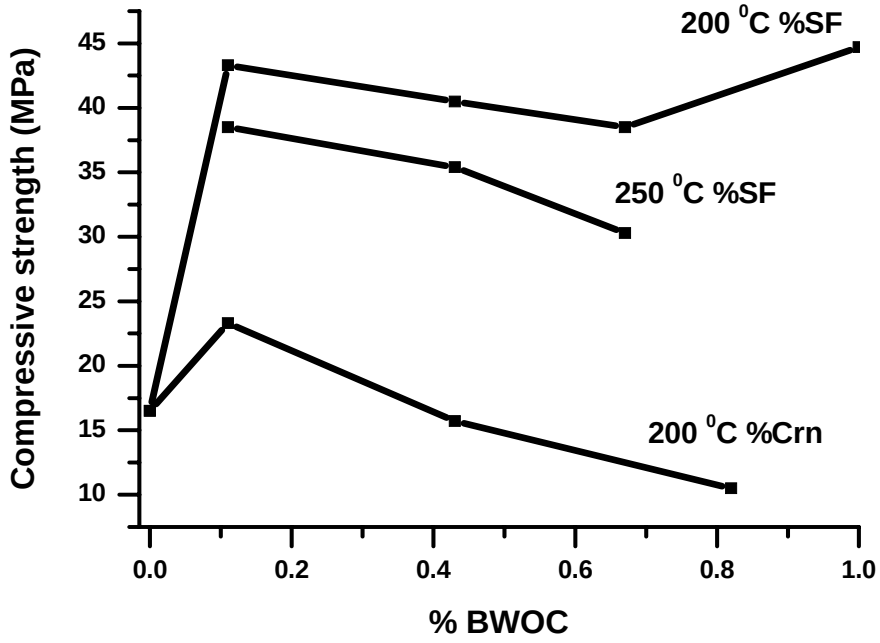

Fig. 3. Plot shows compressive strength against percentage of silica flour and alumina added to hydroceramics for samples cured at 200 °C and 250 °C.

When a small amount of alumina (0.11 BWOC) is added to the system the strength and the permeability are slightly improved. Adding more alumina to the system does not change the mineralogy of the hydroceramics and increasing amounts of unreacted alumina, in the form of corundum, are observed as more than 0.11 BWOC is added (Table 3). The presence of

corundum has an adverse effect on the mechanical properties. We observe a dramatic increase in permeability and decrease in compressive strength (Figs. 3 & 4). Thus the effect of corundum on the physical properties of these hydroceramics appears to be quite different from that of quartz.

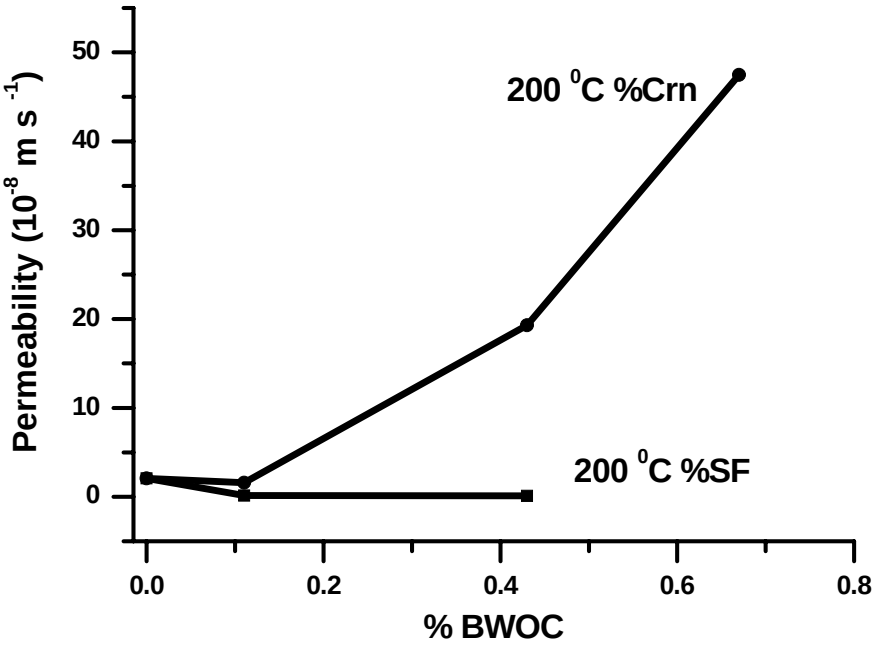

Fig. 4 Graph of permeability against silica and alumina content for samples cured at 200 °C

The mechanical properties of the samples with silica addition cured at 250 °C have also been investigated. The strength of these materials as compared to those cured at 200 °C is lower due to the formation of different minerals. At 250 °C, 0.43 silica BWOC reinhardbraunsite is the major phase instead of C_8S_5 at 200 °C and probably this affects the strength. On increasing the amount of silica, xonotlite appears as before, but 9Å tobermorite and gyrolite are now present, and the strength falls to lower values. It has been reported elsewhere [23] that the formation of gyrolite in autoclaved cement reduces compressive strength.

Comparing our results with permeability data given by Hall & Hoff [24], we see that the permeability of these samples lies between that of clay brick ceramic and that of fine limestone. The permeability of the pure cement system is higher than the cement paste cured at ambient temperature. The reason is that in cement paste cured at ambient temperature the dominant phase is the C-S-H gel. The gel does not have a fine crystallinity therefore it blocks the pores and reduces the permeability. On the other

hand the sample cured at 200 °C is finely crystalline, the C–S–H gel is not present, and there is defined space in the microstructure of the sample (Fig. 2) through which water passes more easily, hence increasing the permeability.

4. Conclusions

This work gives preliminary results on the links between physical properties, microstructure and mineralogy in the CASH hydroceramic system. It appears that the properties of the hydroceramics are improved by adding silica. The new minerals that form (xonotlite, tobermorite) are associated with this improvement. When alumina reacts completely during hydration, forming hydrogarnet, the strength of the sample is improved and the permeability is reduced. In contrast when unreacted alumina in the form of corundum is present the properties deteriorate dramatically.

Further investigations on CASH hydroceramics are in progress. More samples will be tested with different proportions of additives at different temperatures. Also different sources of alumina and silica (such as cenospheres, kaolinite, glass powder) are being added to the system to reduce the presence of relict (unreacted) corundum.

Acknowledgments

We thank EPSRC for funding this research, Robert Hogg and Jane Blackford, School of Engineering and Electronics, The University of Edinburgh, for technical support and useful advice on strength testing and Nicholas Collier and Margaret Carter, School of Mechanical, Aerospace & Civil Engineering, University of Manchester, for help provided during permeability experiments.

References

[1] E. Nelson, Thermal Cements, in: E. Nelson (Eds.), Well Cementing, Schlumberger Educational Services, Sugar Land, Texas, 1990, pp.
[2] R. Oberste-Padtberg, Degradation of Cements by Magnesium Brines, in J. Bayles, G. R. Gouda and A. Nisperos (Eds) Seventh International Conference on Cement Microscopy, International Cement Microscopy Association, 1985
[3] R. A. Kennerly, Products of hydrothermal hydration of cements from geothermal bores, New Zealand Journal of Science 4 (1961) 453-468
[4] J. C. Shen, Effects of CO_2 attack on cement in high temperature applications, Society of Petroleum Engineers (1989)
[5] V. Barlet-Gouédard, S. Danican, E. Nelson and C. Cambus, Cement Compositions for High Temperature Applications, PCT Patent Application WO 03/068708, (21 August 2003)

[6] V. Barlet-Gouédard and B. Goffe, High Temperature Cements, PCT Patent Application WO 2005/040060, (6th May 2005)
[7] N. Meller and C. Hall, Hydroceramic sealants for geothermal wells, in M. Pecchio, F. R. D. Andrade, L. Z. D. D'Agostino, H. Kahn, L. M. Sant'Agostigno and M. M. M. L. Tassinari (Eds) International Congress on Applied Mineralogy, International Council for Applied Mineralogy do Brasil, 2004, 281-284.
[8] N. Meller, C. Hall and J. Phipps, A new phase diagram for the CaO-Al_2O_3-SiO_2-H_2O hydroceramic system at 200^oC, Materials Research Bulletin 40 (2005) 715-723
[9] L. D. Sanders and W. J. Smothers, Effect of tobermorite on the mechanical strength of autoclaves Portland cement-silica mixtures, Journal of the American Concrete Institute 28 (1957) 127-134
[10] E. Nelson and L. H. Eilers, Cementing steamflood and fireflood wells-slurry design, Journal of Canadian Petroleum Technology 25 (1985) 58-63
[11] G. L. Kalousek and S. L. Chow, Research on cements for geothermal and deep oil wells, Society of Petroleum Engineers of AIME SPE 5940 (1976)
[12] G. Carter and D. K. Smith, Properties of cementing compositions at elevated temperatures and pressure, Transactions of the Metallurgical Society of the American Institute of Metallurgical Engineers 213 (1958) 20-27
[13] M. Rowles and B. O. Connor, Chemical optimisation of the compressive strength of aluminosilicate geopolymers synthesized by sodium siliccate activation of metakaolinite, Journal of Materials Chemistry 13 (2003) 1161-1165
[14] S. Sasaki, W. Kobayashi and S. Okabayashi, Strength Development of 2CaO/SiO_2-Silica Cement Undr High-Temperature and High-Pressure Conditions, Society of Petroleum Engineers 1 (1986) 42-48
[15] H. F. W. Taylor, Cement Chemistry, Thomas Telford Publishing, London, 1997
[16] J. Bensted, Developments with oilwell cements, in: J. Bensted and P. Barnes (Eds.), Structure and Performance of Cements, Spon Press, London & New York, 2002, pp. 237-252
[17] Specification for Materials and Testing for Well Cements, American Petroleum Institute, Washington, D.C., 1982
[18] N. Meller, K. Kyritsis, G. Giriat and C. Hall, Synthesis of cement based CaO-Al_2O_3-SiO_2-H_2O (CASH) hydroceramics at 200 and 250^o C: Ex-situ and in-situ diffraction, Cement and Concrete Research (in press)
[19] Annual Book of ASTM Standards, American Society for Testing and Materials, Philadelphia, 1999
[20] K. M. Green, W. D. Hoff, M. A. Carter, M. A. Wilson and J. P. Hyatt, A high pressure permeameter for the measurement of liquid conductivity of porous construction materials, Review of Scientific Instruments 70 (1999) 3397-3401

[21] Recommended practices for core analysis, American Petroleum Institute, Dallas, 1998
[22] V. Barlet-Gouédard and B. Vidick, A non-conventional way of developing cement slurry for geothermal wells, Geothermal Resources Council Transactions 25 (2001) 85-91
[23] N. Isu, H. Ishida and T. Mitsuda, Influence of quartz particle size on the chemical and mechanical properties of autoclaved aerated concrete (I) Tobermorite formation, Cement and Concrete Research 25 (1995) 243-248
[24] C. Hall and W. D. Hoff, Water transport in brick, stone and concrete, Spon Press, London, 2002